Scientific Review Engineering and Environmental Sciences (2023), 32 (2), 135–154

Sci. Rev. Eng. Env. Sci. (2023), 32 (2) https://srees.sggw.edu.pl

ISSN 1732-9353 (suspended) eISSN 2543-7496 DOI 10.22630/srees.4548

Received: 19.11.2023
Accepted: 28.03.2023

Rafi Mohammed QASIM https://orcid.org/0000-0002-1882-0766
Tahseen Ali JABBAR https://orcid.org/0000-0002-0602-9627
Safaa Hameed FAISAL✉ https://orcid.org/0000-0002-7752-9071
Southern Technical University, Basra Engineering Technical College, Basra, Iraq

Simulation of laminar flow passing through a T-splitter plate and bridge pier

Keywords: hydrodynamic laminar flow, open channel, pier, splitter plate

Introduction

The flow around the pier represents a serious subject due to the direct relationship between the structural hydraulic collapse and the stability of the upper structure, which is supported by the pier. The erosion in the soil particle depends mainly on the flow velocity, water depth and the size of the soil particle. Here, the flow velocity has a major impact on the erosion process regardless of the type of flow as compared with the remaining previous factors. Therefore, the type of flow has a direct influence on the stability of mobile material (soil bed). Here, the hydraulic designer encounters a noticeable challenge based on how we satisfy a reasonable balance between a huge hydraulic field and the structural resistance to this hydraulic field without any negative aspect on the serviceability life of the pier. However, to protect the pier against the hydraulic field, several ways must be applied to produce a proper equilibrium between the hydraulic field and pier stability, therefore

✉s_hfaisal100@stu.edu.iq

this problem gives evidence regarding the risk that may occur when the hydraulic field suddenly alters its behavior. Several papers dealt with water fields around the pier. Here, we mention some of these significant papers. In general, the previous paper adopted a splitter plate with a rectangular shape. The rectangular shape will divide the flow in two directions along the solid boundary side of the plate. Thus, only the separation process will be developed at the corner edge of the rectangular shape and these separation points constitute fixed separation points. The authors suggest duplicating the separation process with the dissipation process, therefore they use the T-shaped splitter plate. The T-shaped splitter plate consists of two parts; the first part is longitudinal, which is parallel to the flow direction, while the second part is transverse, which is perpendicular to the flow direction. Here, the expected dissipation process will occur largely in the second part in addition to the separation process, which occurs at the corner edge of the second part. Qasim, Jabbar and Abdulhussein (2022a), Jabbar, Qasim and Mohammed (2022a), as well Qasim and Jabbar (2021) tried to produce safe hydrodynamic fields around a pier by installing a vane at the upstream part of the pier. These efforts gave a good indicator regarding the way we dominate the hydrodynamic field and this is shown clearly in the reduction, which is earned especially in the drag coefficient. Furthermore, these papers dealt with several hydraulic parameters and implied how the vane made the reduction in these parameters at a feasible level. Shen, Lin, Wei, Dou and Tu (2019) achieved an experimental work to reveal the characteristics of the vortex shedding behind a cylinder under the impact of the flexible film, in this experimental study the ratio of the flexible film length to the cylinder diameter L/D and Reynolds number is increased. This research focused on efforts to identify the effect of the flexible film flapping with various L/D parameters on the distribution of the fluctuation pressure and the vortex shedding frequency. Hu and Wang (2013) used the particle imaging velocimetry (PIV) to study the structure of the flow around an oscillating cylinder attached to a flexible tail. The paper concentrated on the flow velocity along the wake center line as well as the vertical flow velocity around the flexible tail trailing edge. Shukla, Govardhan and Arakeri (2013) investigated the issue of a flexible splitter plate in the wake of a cylinder experimentally; the plate flexural rigidity has been adopted in the investigation. Meanwhile, the Reynolds number value depends on the cylinder diameter. Periodic splitter plate motions are shown to exist in two regimes. Ahmed (2015) conducted a numerical analysis of vortex shedding while taking laminar flow with $30 \leq \mathrm{Re} \leq 300$ into consideration. The numerical solution of the hydraulic issue uses two-dimensional, incompressible, and unsteady flow. The results also showed that the flow is asymmetric and unsteady at Reynolds numbers over 60, and

a strong comparison could be made between the findings with those of studies that were conducted earlier. Govardhan and Williamson (2000), as well as Carberry, Sheridan and Rockwell (2005), discovered the mechanism that started the changes in the phase and amplitude of the lift force, also the relations with the mod of vortex shedding. Mehdi, Namdev, Kumar and Tyagi (2016) performed a numerical solution in two-dimensions to study the flow around a cylinder. Here, three values of the Reynolds number are used, which are 1,000, 500, and 200 with various values of attack angles 10°, 5°, and 0°. The numerical investigation concentrated on vortex shedding, drag coefficient, and pressure. Bai and Li (2011) implemented a two dimensional flow analysis around the cylinder numerically for seeking the hydrodynamic pattern characteristics. The flow is simulated as unsteady, uniform, and laminar. The study focused on the Strouhal number, lift coefficient, drag coefficient, and pressure distribution, the study adopted Re = 200. Dennis and Chang (1970) utilized the formulation of stream-vorticity and discretization of finite difference to find a solution for a steady incompressible flow across the cylinder up to Re = 100. Henderson (1995) utilized the spectral element method to calculate the base pressure, pressure drag, and viscous drag for the flow around a cylinder, which has a circular cross-section. Recently, Qasim, Jabbar and Faisal (2022b) have investigated the hydrodynamic field response of a cylindrical pier due to using a curved vane with the assumption of a laminar flow. They observed alteration in the direction of the flow velocity, especially at the leading and rear surfaces of the curved vane due to the existence of flow separation and dissipation along the boundary of the vane. Jabbar, Qasim and Faisal (2022b) studied the flow characteristics around a circular pier that adjacent T-shape splitter in a numerical manner. The analysis includes vortex's length, streamlines, flow velocity contour, and pressure contour. They found that the streamlines, flow velocity field, and pressure field are affected mainly by the horizontal distance between the rear part of the splitter and the pier center. In addition, the Re number will directly control the streamlines, flow field, and pressure field. Qasim, Faisal and Jabbar (2022c) introduced another study about the hydrodynamic behavior surrounding the pier near a T-shape splitter. The study covers water velocity contours, pressure contours, and streamlines. Results reveal that bubbles are developed due to the presence of the splitter and the size and length of these bubbles are controlled by the Reynolds number.

The aim of this paper can be summarized into the following points:

1. Investigate the velocity vector around a bridge pier to understand the direction of water flow due to the existence of a T-splitter plate. Here, various values of the Reynolds number are used with a constant value of ratio X (ratio X is defined later in the next section).

Qasim, R. M., Jabbar, T. A., Faisal, S. H. (2023). Simulation of laminar flow passing through a T-splitter plate and bridge pier. *Sci. Rev. Eng. Env. Sci.*, *32* (2), 135–154. DOI 10.22630/srees.4548

2. Investigate the drag coefficient and lift coefficient for two different cases, considering various values of the Reynolds number and horizontal distance between the leading part of the pier and the rear part of T-splitter plate.

3. Investigate the skin friction coefficient for two different cases, considering various values of Reynolds number and horizontal distance between the leading part of the pier and the rear part of T-splitter plate.

Methodology

The entire hydraulic problem comprises of three parts, which are the fluid, a circular pier, and a T-shaped splitter plate. The numerical model is accomplished in two dimensions and the flow is considered to be laminar. The values of the Reynolds number, which is used to implement the hydraulic analysis, are 40, 80, 120, and 200. The calculated Reynolds number is based on the pier diameter and flow velocity. The stream flow of water starts from the left, first crosses the T-splitter, and then moves towards the circular pier. The hydraulic analysis deals with two different cases, which are illustrated in Figure 1. Furthermore, Figure 1 depicts the hydraulic dimensions of the fluid domain. Here, the T-splitter plate produces

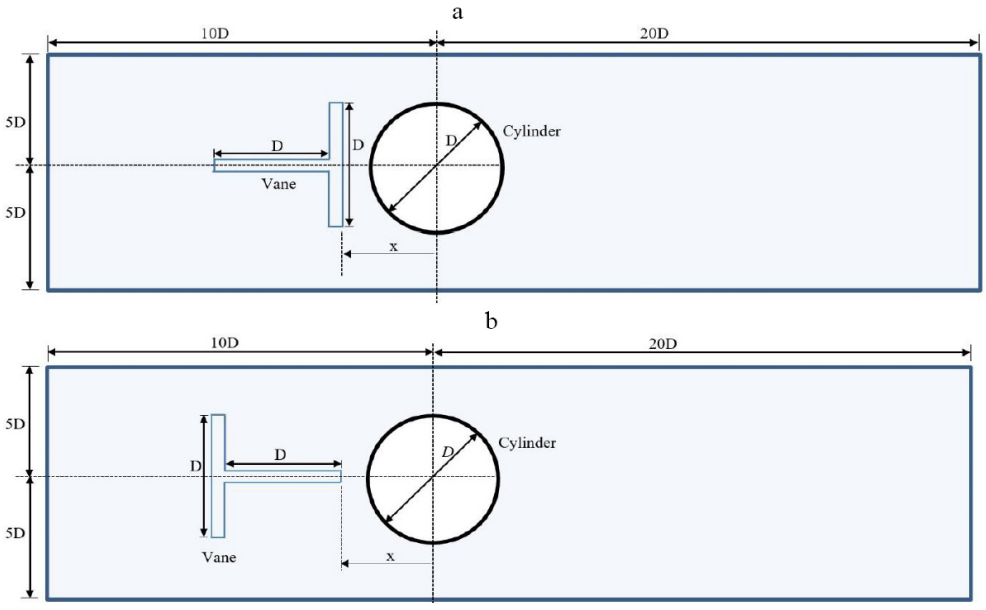

FIGURE 1. The hydraulic domain including the cylinder and T-splitter plate: a – Case 1; b – Case 2
Source: own work.

a deformation to the water flow when the flow passes the splitter, therefore the flow field around the pier is always changing based on flow separation and dissipation. The T-splitter plate arm's dimensions are equal to the diameter of the pier. Various locations of T-splitter plate reference to the location of the pier are investigated in the current study. Here, x refers to the horizontal distance from the pier center to the rear part of the splitter plate.

The steady flow analysis is implemented by ANSYS Fluent and in all cases, the splitter plate is considered to be rigid. The governing equations that will be used for the simulation and solved by the software are incompressible fluid continuity equation and the conservation of momentum equation as given in Eqs (1)–(3), (Dahkil, Gabbar & Jaber, 2014; Sharma & Barman, 2020).

$$u\frac{\partial u}{\partial x}+v\frac{\partial u}{\partial y}=-\frac{1}{\rho}\frac{\partial P}{\partial x}+\frac{\mu}{\rho}\left(\frac{\partial^2 u}{\partial x^2}+\frac{\partial^2 u}{\partial y^2}\right). \tag{1}$$

$$u\frac{\partial v}{\partial x}+v\frac{\partial v}{\partial y}=-\frac{1}{\rho}\frac{\partial P}{\partial y}+\frac{\mu}{\rho}\left(\frac{\partial^2 v}{\partial x^2}+\frac{\partial^2 v}{\partial y^2}\right). \tag{2}$$

$$\frac{\partial(u)}{\partial x}+\frac{\partial(v)}{\partial y}=0. \tag{3}$$

The calculations are performed using the default commercial CFD code in ANSYS Fluent 2020 R1. The feeding information submitted to the fluent software is the inlet flow velocity, while the output data includes the flow velocity components and the pressure magnitude. The discretization equations are solved using the semi-implicit method for pressure-linked equations (SIMPLE) method and formula from the upwind scheme. Furthermore, the convergence criteria is 1E – 4 for momentum equations and 1E – 6 for energy equation. The simulation was performed with an 8 GB RAM Intel Core i7 processor.

The drag coefficient (CD) is defined as:

$$CD=\frac{F_D}{\frac{1}{2}\rho U_\infty^2 A_{ref}}, \tag{4}$$

where F_D is the drag force, U_∞ is the free-stream velocity, and A_{ref} is the reference area. The reference area in this case is the projection area, which is equal to the diameter for the unit depth.

Qasim, R. M., Jabbar, T. A., Faisal, S. H. (2023). Simulation of laminar flow passing through a T-splitter plate and bridge pier. *Sci. Rev. Eng. Env. Sci.*, *32* (2), 135–154. DOI 10.22630/srees.4548

Concerning lift coefficient (CL) is defined by:

$$CL = \frac{F_L}{\frac{1}{2}\rho U_\infty^2 A_{ref}}, \tag{5}$$

where F_L is the lift force. The reference area (wing area) is also equal to the diameter for unit depth.

The skin friction factor is obtained from the formula:

$$Cf = \frac{\tau_L}{\frac{1}{2}\rho U_\infty^2}, \tag{6}$$

where τ_L is the shear stress at the wall.

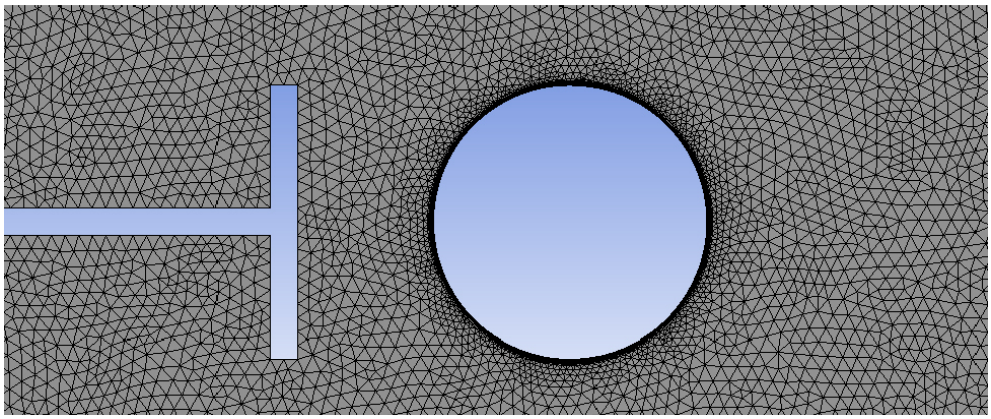

FIGURE 2. Mesh geometry of Case 1
Source: own work.

The element specifications adopted in this study are: the number of the element is 71,566 elements for Case 1 and 71,267 elements for Case 2, triangle mesh type, and the diameter of the cylinder-to-element size ratio of 20. Figure 2 shows the mesh of Case 1 and Table 1 illustrates the boundary conditions applied for the entire hydraulic system. The mesh is

TABLE 1. Boundary conditions

Inlet	Velocity
Outlet	pressure
T-splitter and pier	no-slip
Channel bed and sides	no-slip

Source: own work.

concentrated highly around the pier and the splitter plate. The smooth mesh is employed for both cases. The properties of water are taken as ρ = 997.1 kg·m^{-3} and μ = 89.05E – 5 kg·s^{-1}·m^{-1}.

Referring to Figure 1, the ratio X is defined as:

$$X = \frac{x}{D}, \tag{7}$$

where x is the horizontal distance between the leading part of the pier and the rear part of the T-splitter plate. The pier diameter is denoted by D.

Validation

It is very important to check the effectiveness of the used software. Here, before solving the current problem, we check the software by adopting a previous case study performed by Rajani, Kandasamy and Majumdar (2009). Depending on the comparative study between the result of the previous paper and the current result, it is apparent that there is no fluctuation among the results. Therefore, we can now start the required analysis of the current hydraulic problem. Figure 3 reveals that the separation angle decreases with the increase of the Reynolds number. Both studies (previous and current) are achieved in a two-dimensional flow analysis.

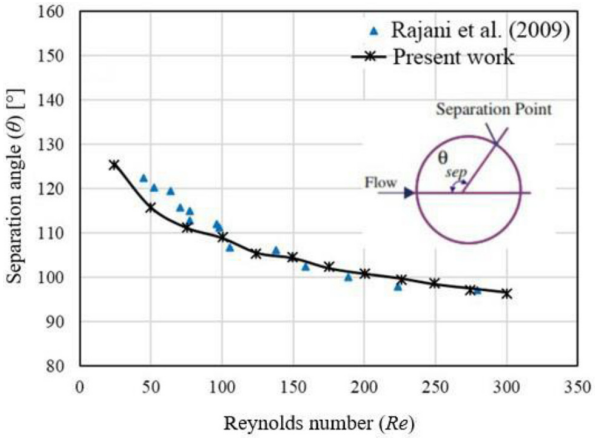

FIGURE 3. The variation of separation angle (θ) with Reynolds number (Re)
Source: own work.

Qasim, R. M., Jabbar, T. A., Faisal, S. H. (2023). Simulation of laminar flow passing through a T-splitter plate and bridge pier. *Sci. Rev. Eng. Env. Sci.*, *32* (2), 135–154. DOI 10.22630/srees.4548

Results and discussion

In this paper, two different cases have been investigated and compared. The target is to show the direct influence of the splitter plate on the hydrodynamic patterns around the bridge pier. The hydraulic problem is analyzed by adopting fluid with the same physical properties for both cases. Here, water is the flow material around the splitter plate and pier. Figure 4 shows the velocity vector for Case 1 considering Re and ratio X. We take four points to understand the velocity vector behavior, two approximately counterpoints located at the leading portion of the pier or in other words these two points fall on the boundary layer zone while the other counterpoints located at the rear portion of the pier or fall on the wake zone. For the case Re = 40 and X = 1.2, for points at the leading of the pier, we notice the flow is divided into two portions. Here, a portion goes toward the zone between the splitter plate and the pier leading portion while the remaining flow portion goes toward the wake zone. Now, for points at the rear of the pier, we noticed that flow comes from the boundary layer zone combined with the flow at the rear of the pier and goes toward the hydraulic system downstream. The same hydraulic behavior remains without any alteration for the following cases Re = 80 and ratio X = 1.2 and Re = 140 and ratio X = 1.2. When Re becomes 200 and the ratio X is constant, dramatic hydraulic behavior in the flow will take place, here, we investigate the flow at the pier circumference on both sides along the boundary zone and wake zone. We find that the flow at the wake zone tends to move towards the boundary zone, while a small quantity of flow moves towards the downstream of the pier. We must bring to light two different processes, which happened to the flow stream before crossing the rear portion of the splitter plate. These processes are separation and dissipation processes. In Case 1 the flow will first be separated by the longitudinal splitter plate and then the flow will be reflected by the transverse splitter plate. Here, the flow velocity will vary due to the unbalanced processes that occurred to the flow velocity at the splitter plate. Therefore, the flow suffers from the losses in energy and changing in its direction. Therefore, some water goes to fill the gap (distance) between the rear portion of the splitter plate and the leading portion of the bridge pier while the remainder goes toward the wake zone. Now for the flow between the splitter plate and the pier, at the pier boundary layer zone, the flow suffered from losses in kinetic energy or losses in the flow velocity. Moreover, some flow recirculates to the wake zone and some recirculates in the zone between the rear portion of the splitter plate and the leading portion of the pier, as well this flow will suffer from the losses in the flow velocity. The value of the Reynolds number will contribute to the disturbance of the flow velocity vector. With the rise in Reynolds number value, the water flow suffered tremendous changes in the flow velocity magnitude and direction.

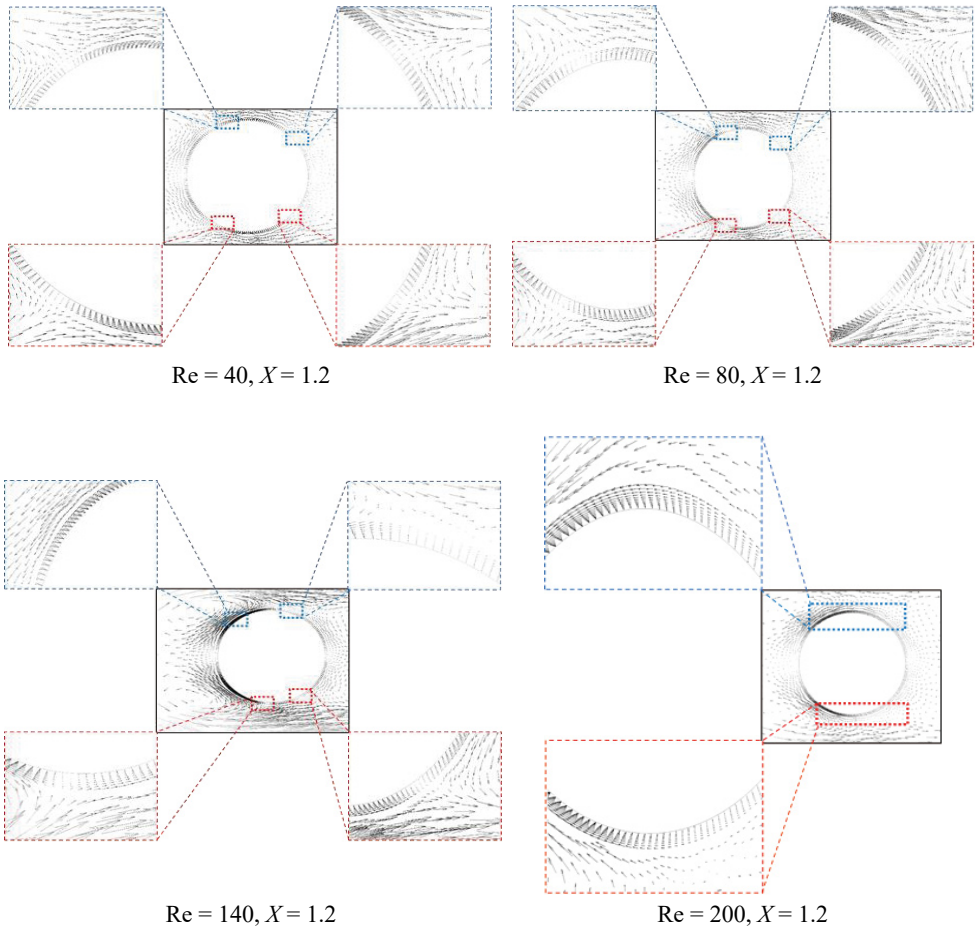

FIGURE 4. Indicates the velocity vector for Case 1
Source: own work.

Figure 5 shows the velocity vector for Case 2 considering Re and the ratio *X*. The same procedure, which is adopted in Case 1 is employed to investigate Case 2. When Re = 40 and Re = 80 with a constant value of ratio *X*, the hydraulic behavior in Case 2 is similar to the hydraulic behavior of Case 1, while when Re = 140 and Re = 200 with a constant value of the ratio *X* there is no identically in the hydraulic behavior, i.e with the increase in flow velocity, the hydraulic behavior will be changed according to the magnitude of velocity. Here, approximately the entire flow diverted its direction toward the gap (distance) between the leading portion of the pier and the rear portion of the splitter plate. For this event, the water flow suffered from the separation process

Qasim, R. M., Jabbar, T. A., Faisal, S. H. (2023). Simulation of laminar flow passing through a T-splitter plate and bridge pier. *Sci. Rev. Eng. Env. Sci.*, *32* (2), 135–154. DOI 10.22630/srees.4548

at the splitter plate and losing (shortages) of the kinetic energy at the circumference of the pier leading portion. The remaining flow goes immediately towards the wake zone.

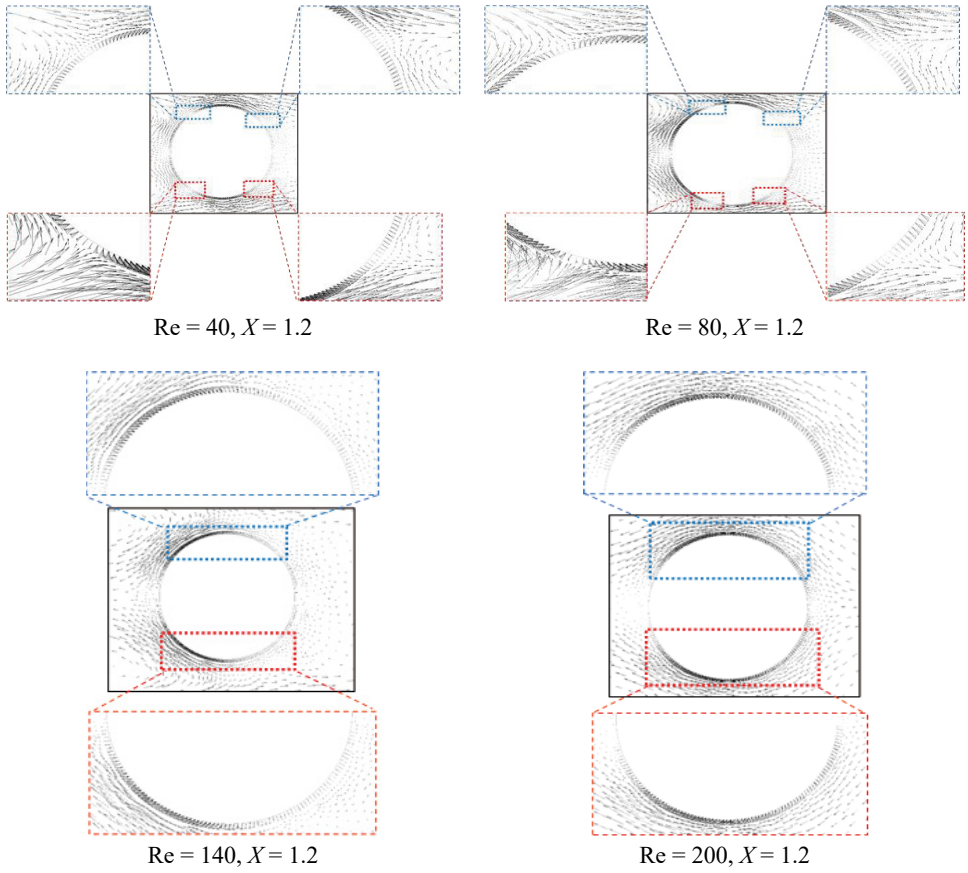

FIGURE 5. Indicates the velocity vector for Case 2
Source: own work.

The variation of the drag coefficient ratio of the bridge pier with the ratio X is outlined in Figure 6. From the figure, we can infer that the drag coefficient of the pier nearby the T-splitter plate is less than the drag coefficient of the pier alone. A nonlinear trend in relation is found among various values of the drag coefficient ratio with the ratio X. In spite of the variation in the Reynolds number values, negative drag coefficient values are found regardless of the values of the ratio X. On the front surface

of the pier, the stagnation pressure is reduced due to the existence of the upstream T-splitter plate. When the pressure is reduced, the flow velocity will rise and this rising leads to a reduction in the drag coefficient. The figure shows that there is a slight variation in the curve trend when Re = 140 and Re = 200 as compared to the others. In addition, the variation in the lift coefficient ratio of the bridge pier with the ratio X is outlined in Figure 7. The values of the lift coefficient vary among negative values and positive values with various values of the ratio X. It is shown that no dramatic change in the lift coefficient values regardless of the values of the Reynolds numbers and all the obtained values of the lift coefficient are close together. From Figures 6 and 7, we can conclude that as the drag coefficient increases, the lift coefficient decreases. In the laminar flow, negative lift coefficients exist due to the low angle of attack.

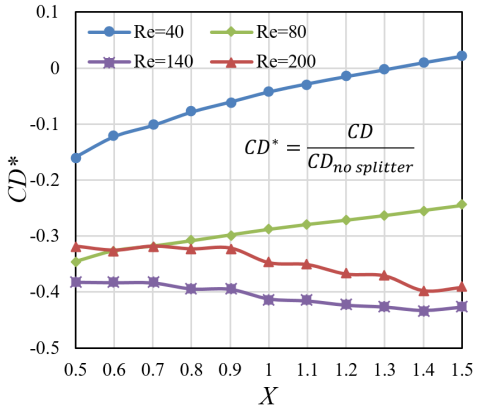

FIGURE 6. Drag coefficient (CD*) for Case 1
Source: own work.

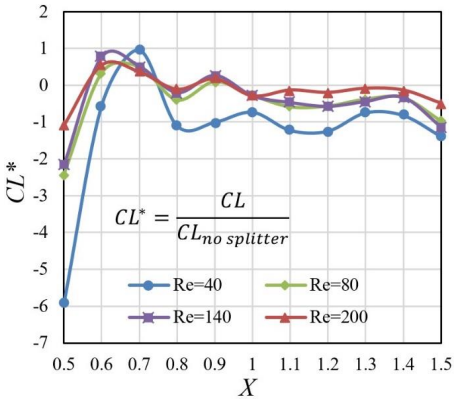

FIGURE 7. Lift coefficient (CL*) for Case 1
Source: own work.

Figures 6 and 7 are drawn for Case 1. For Case 2, Figure 8 illustrates the variation in the drag coefficient ratio with the ratio X for various values of the Reynolds numbers. The behavior of the drag coefficient for Case 2 is similar to the behavior of Case 1 except that the trend in Case 2 varied in terms of the linear and non-linear aspect. The alteration in trend relies on the flow velocity. Here, the flow velocity is based on the separation and dissipation processes and which one will occur first. Figure 9 illustrates the variation in the lift coefficient ratio with the ratio X for various values of the Reynolds numbers. It is clear from Figure 9 that all values of the lift coefficient are equal to or approximate to zero, this is due to shortages in the flow mass, which produce the lift in the pier.

Qasim, R. M., Jabbar, T. A., Faisal, S. H. (2023). Simulation of laminar flow passing through a T-splitter plate and bridge pier. *Sci. Rev. Eng. Env. Sci.*, *32* (2), 135–154. DOI 10.22630/srees.4548

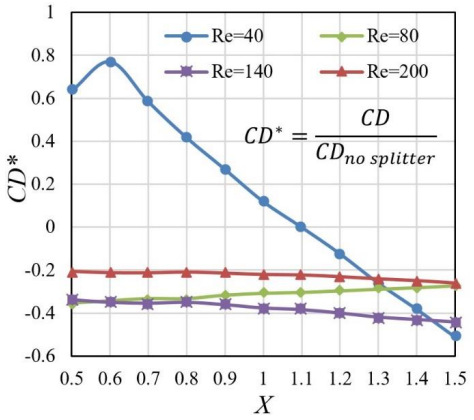

FIGURE 8. Drag coefficient (*CD**) for Case 2
Source: own work.

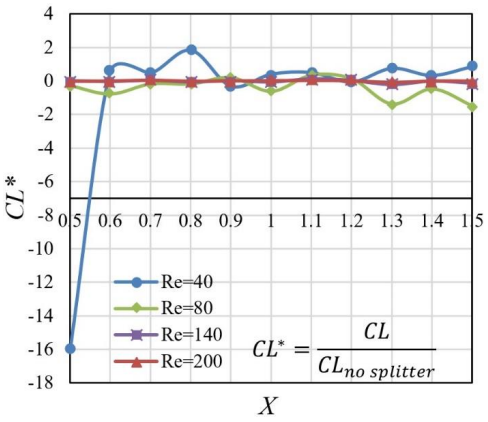

FIGURE 9. Lift coefficient (*CL**) for Case 2
Source: own work.

Figure 10 reveals a comparative study between the drag coefficient ratio of the two cases taking into consideration four different values of the Reynolds number and various values of the ratio *X*. The argument here relies on the fact which processes occur at the leading portion of the T-splitter plate, leading portion of the pier, and rear portion of the T-splitter plate. In addition, the kinetic energy flow suffers losses. From the figure, for Re = 40, the curve of Case 1 has a moderate trend while the curve of the Case 2 drops sharply from positive values to negative values without any contrast. When Re = 80, the curves of both cases rise dramatically without any variation. Also, when Re = 140 and Re = 200 both curves drop sharply without any fluctuation. From Figure 10 we can deduce the benefit of installing a splitter plate at the upstream of the bridge pier in order to reduce the drag coefficient and produce a suitable flow field around the pier to prevent pier collapse under hydraulic loading and keep safe applied hydraulic loading.

Figure 11 is drawn to express the relation between the skin friction coefficient ratio and the ratio *X* for different values of the Reynolds numbers. We deduce that the skin friction of the bridge pier alone is greater than the skin friction of the bridge pier nearby the splitter plate. It is obvious from the Figure as the ratio *X* increases, the skin friction coefficient increases as well regardless of the value of the Reynolds number. In general, skin friction or skin friction drag is caused by fluid viscosity and relies on flow velocity and the projection area of the pier that has direct contact with the fluid. For the contact area in case of the splitter plate existence or without splitter plate existence, the area is always constant. Here, the flow velocity has a vital role in determining the skin friction value. When the Reynolds number increases, it

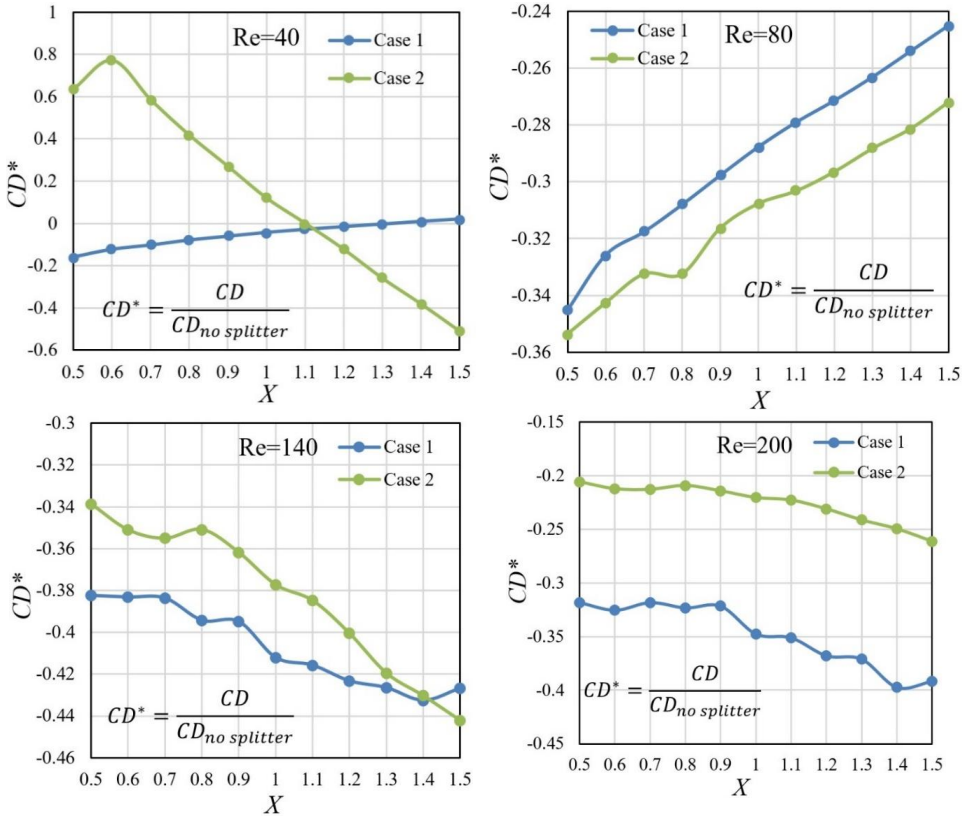

FIGURE 10. Variation of drag coefficient (CD^*) with the ratio X for various values of Reynolds number (Re)

Source: own work.

means that the viscous force will decrease together with the skin friction coefficient. Therefore, the Reynolds number is independent of the skin friction, this situation is clear in the figure, at Re = 40 where the blue curve represents the upper limit, while the remaining curves of Re greater than 40 fall under the curve which has Re = 40. Moreover, laminar sub-layer thickness decreases with an increase in the Reynolds numbers values. All curves in Figure 11 have a nonlinear trend.

Figure 12 shows the variation in relation between the skin friction ratio and different Reynolds numbers values for three different values of the ratio X. It is evident from the figure as the Reynolds number increases, the skin friction ratio decreases and this condition is discussed in the previous section but here we noticed that the distance between the splitter plate and the bridge pier does not affect the skin friction value. That is because skin friction depends directly on fluid viscosity and flow

Qasim, R. M., Jabbar, T. A., Faisal, S. H. (2023). Simulation of laminar flow passing through a T-splitter plate and bridge pier. *Sci. Rev. Eng. Env. Sci.*, *32* (2), 135–154. DOI 10.22630/srees.4548

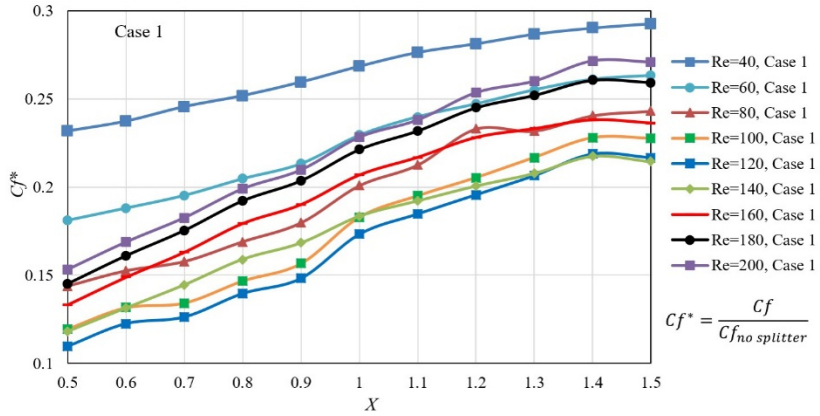

FIGURE 11. Relation between skin friction ratio (*Cf**) and ratio *X* for Case 1

Source: own work.

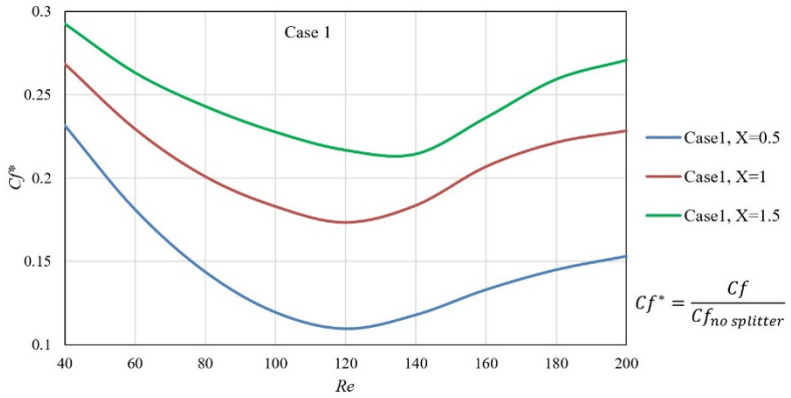

FIGURE 12. Relation between skin friction ratio (*Cf**) and Reynolds numbers (Re) for Case 1

Source: own work.

velocity magnitude. Also, we can see from the figure a nonlinear trend in the relation between the Reynolds numbers and the skin friction ratio.

Figure 13 and Figure 14 are drawn for Case 2. Figure 13 is outlined to express the relation between the skin friction coefficient ratio and the ratio *X* for different values of the Reynolds numbers. Figure 14 shows the variation in relation between skin friction ratio and different Reynolds numbers values for three different values of the ratio *X*. In both figures, the hydraulic behavior of Case 2 is similar to the hydraulic behavior of Case 1 regardless of the configuration of the T-splitter plate. All the curves in Figure 14 have a harmonic trend as compared with curves in Figure 12, this feature is attributed to the flow velocity magnitude.

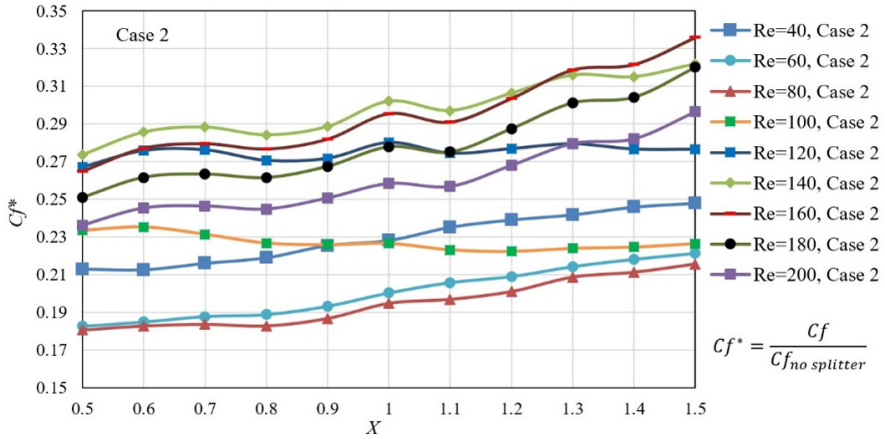

FIGURE 13. Relation between skin friction ratio (Cf^*) and ratio X for Case 2
Source: own work.

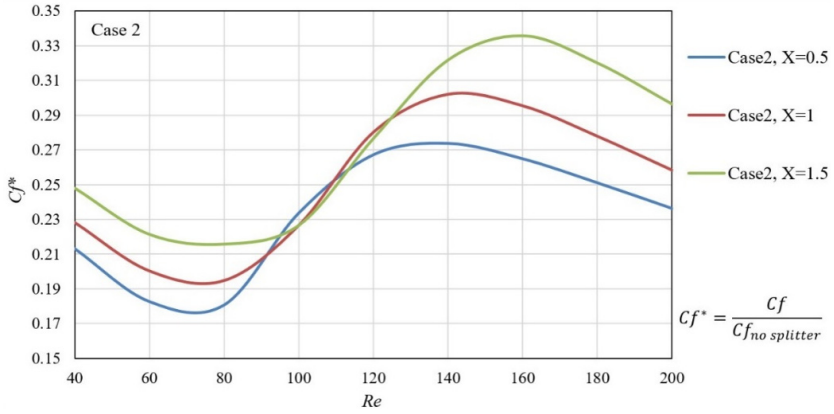

FIGURE 14. Relation between skin friction ratio (Cf^*) and Reynolds number (Re) for Case 2
Source: own work.

Figure 15 reveals the relation between the skin friction coefficient and the Reynolds number for both cases (1 and 2) considering various values of the ratio X. When the ratio X is equal to 0.5 and 0.6, the curve of Case 1 and the curve of Case 2 intersect at Re = 60 and Cf^*. When the ratio X is equal to 0.7, 0.8, and 0.9, the curves of both cases intersect at Re between 60 and 80 and Cf^* between 0.18 and 0.183. While the ratio X values become 1 to 1.5, the curves of both cases intersect at Re between 80 and 100 and Cf^* between 0.19 and 0.23. The contrasts in skin friction ratio values appear to some extent. Therefore, it can be deduced that the skin friction is considered independent and the values of the skin friction do not depend

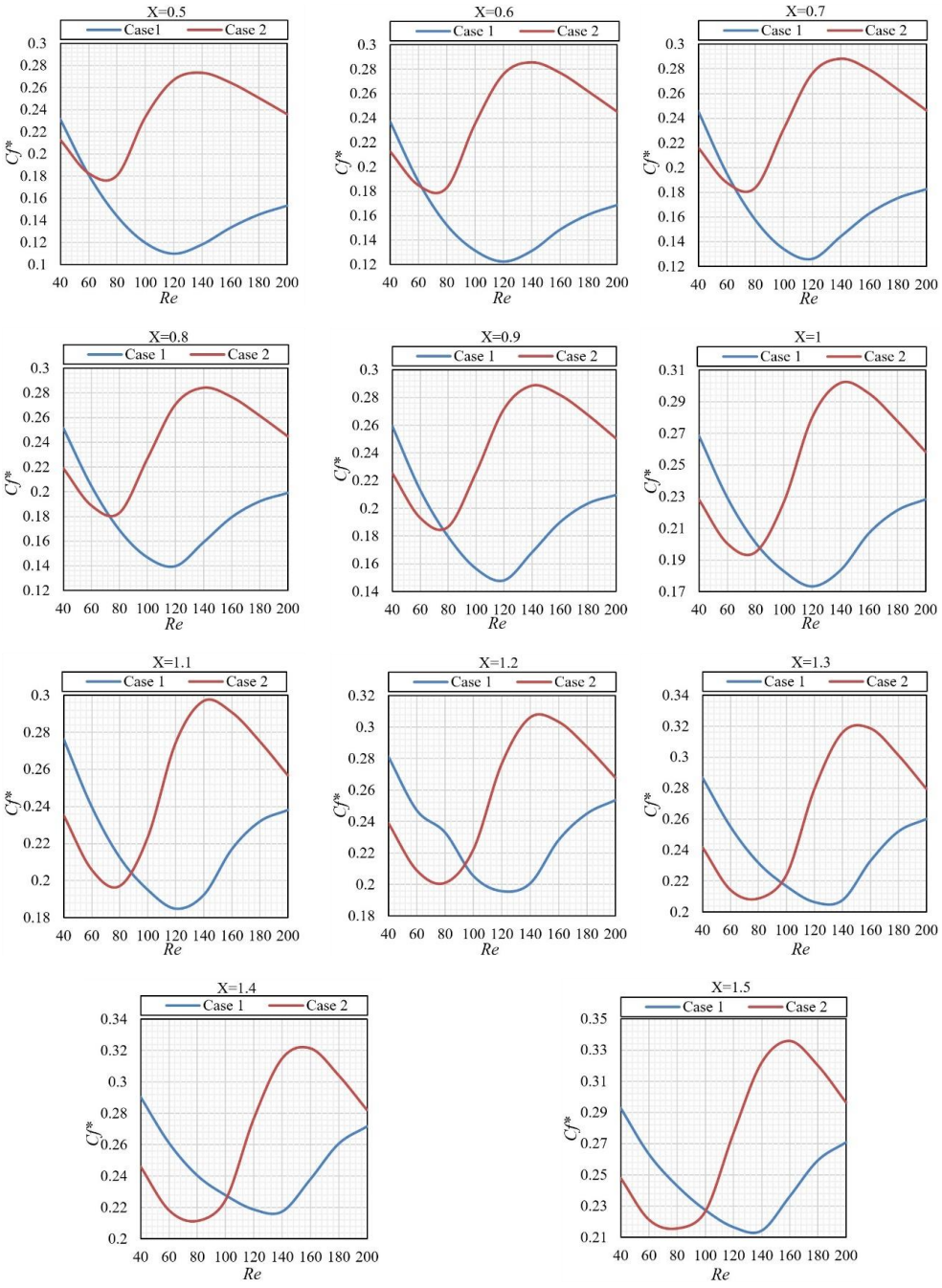

FIGURE 15. The variation in skin friction ration (*Cf**) with Reynolds number (Re) for different values of the ratio *X*

Source: own work.

on the Reynolds numbers and the horizontal distance between the bridge pier and the T-splitter plate.

From the numerical analysis and based on the same value of Cf^* for both cases, a theoretical equation comprises the Reynolds numbers values and the values of the ratio X are obtained. Figure 16 shows the trend of this theoretical equation. The equation has a nonlinear trend with the highest degree equal to a third degree:

$$\mathrm{Re} = A X^3 + B X^2 + C X + D. \tag{8}$$

The values of A, B, C and D are indicated in Figure 16.

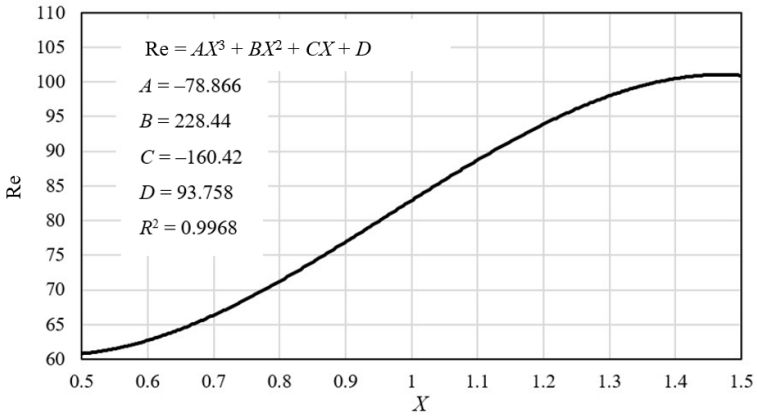

FIGURE 16. The relationship between Reynolds number (Re) and ratio X at same skin friction ratio (Cf^*) for both cases

Source: own work.

Conclusions

In this work, we considered a water-T-shaped splitter plate – water – bridge pier as a new idea in the fluid – structure problem. The influence of the Reynolds number or flow velocity on the hydrodynamic field around the hydraulic system which consists of the three parts (water, T-splitter plate, and pier) has been analysed. So, the following major points have been inferred from this hydraulic analysis. The values of the drag coefficient, lift coefficient, and skin friction coefficient of the pier alone are higher than the corresponding values when the splitter plate exists. The fundamental role of the splitter plate existence is to dominate the flow velocity field around the

pier. In addition, the splitter plate works as a tool to control the separation and dissipation processes at the front of the pier. Also, a nonlinear trend in relation is found among various values of the drag coefficient ratio with the ratio *X* regardless of the values of the Reynolds numbers. It is found that the skin friction coefficient has an inversely proportional relationship with the Reynolds number values and horizontal distance between the pier and the rear portion of the splitter plate. Moreover, the results show that there is no direct or measured relationship between the drag coefficient and lift coefficient due to the following reasons, the drag coefficient depends on the projection area which is perpendicular to the flow area while the lift coefficient depends on the area which is parallel to flow in spite of both coefficients depend on the flow velocity. The flow velocity gradient has a major impact on the values of the skin friction factor. Here, we must mention that the flow velocity gradient has direct proportionality with the shear stress, which is developed and grow at the skin of the pier and this will be reflected directly on the value of the skin friction factor.

References

Ahmed, R. A. (2015). Simulation of unsteady flow around a cylinder. *Wasit Journal of Engineering Sciences*, *3* (2), 28–49. https://doi.org/10.31185/ejuow.vol3.iss2.38

Bai, H. & Li, J. W. (2011). Numerical simulation of flow over a circular cylinder at low Reynolds number. *Advanced Materials Research*, *255–260*, 942–946. https://doi.org/10.4028/www.scientific.net/amr.255-260.942

Carberry, J., Sheridan, J. & Rockwell, D. (2005). Controlled oscillations of a cylinder: forces and wake modes. *Journal of Fluid Mechanics*, *538*, 31–69. https://doi.org/10.1017/s0022112005005197

Dahkil, S. F., Gabbar, T. A. & Jaber, D. K. (2014). Numerical study of the initial pressure and diameters ratio effect on the jet ejector performance. *Basrah Journal for Engineering Science*, *14* (1), 122–135.

Dennis, S. C. R. & Chang, G. Z. (1970). Numerical solutions for steady flow past a circular cylinder at Reynolds numbers up to 100. *Journal of Fluid Mechanics*, *42* (3), 471–489. https://doi.org/10.1017/s0022112070001428

Govardhan, R. & Williamson, C. H. K. (2000). Modes of vortex formation and frequency response of a freely vibrating cylinder. *Journal of Fluid Mechanics*, *420*, 85–130. https://doi.org/10.1017/s0022112000001233

Henderson, R. D. (1995). Details of the drag curve near the onset of vortex shedding. *Physics of Fluids*, *7* (9), 2102–2104. https://doi.org/10.1063/1.868459

Hu, Y. & Wang, J. (2013). The effects of attached flexible tail length on the flow structure of an oscillating cylinder. *Science China Physics, Mechanics and Astronomy*, *56* (2), 340–352. https://doi.org/10.1007/s11433-013-5014-8

Jabbar, T. A., Qasim, R. M. & Faisal, S. H. (2022b). Effect of T-shape splitter on the hydraulic response of the bridge pier. *U.P.B. Scientific Bulletin, Series D*, *84* (4), 263–280.

Jabbar, T., Qasim, R. & Mohammed, B. (2022a). The impact of the vane angle on the hydraulic behaviour around the cylinder. In *Proceedings of 2nd International Multi-Disciplinary Conference Theme: Integrated Sciences and Technologies*, IMDC-IST 2021, 7–9 September 2021, Sakarya, Turkey. https://doi.org/10.4108/eai.7-9-2021.2315298

Mehdi, H., Namdev, V., Kumar, P. & Tyagi, A. (2016). Numerical analysis of fluid flow around a circular cylinder at low Reynolds number. *IOSR Journal of Mechanical and Civil Engineering (IOSR-JMCE)*, *13* (3), 94–101.

Qasim, R. M. & Jabbar, T. A. (2021). An analytic study of the effect of a vane on the hydraulic field around a cylinder. *INCAS BULLETIN*, *13* (3), 123–139. https://doi.org/10.13111/2066-8201.2021.13.3.11

Qasim, R., Jabbar, T. & Abdulhussein, I. (2022a). Flow field simulation between angle vane and cylinder. In *Proceedings of 2nd International Multi-Disciplinary Conference Theme: Integrated Sciences and Technologies*, IMDC-IST 2021, 7–9 September 2021, Sakarya, Turkey. https://doi.org/10.4108/eai.7-9-2021.2315181

Qasim, R. M., Jabbar, T .A. & Faisal, S. H. (2022b). Effect of the curved vane on the hydraulic response of the bridge pier. *Ocean Systems Engineering*, *12* (3), 335–358. https://doi.org/10.12989/ose.2022.12.3.335

Qasim, R. M., Faisal, S. H. & Jabbar, T. A. (2022c). Impact of T-splitter on the laminar flow field around cylinder pier. *Advances in Science and Technology Research Journal*, *16* (5), 202–215. https://doi.org/10.12913/22998624/154795

Rajani, B. N., Kandasamy, A. & Majumdar, S. (2009). Numerical simulation of laminar flow past a circular cylinder. *Applied Mathematical Modelling*, *33* (3), 1228–1247. https://doi.org/10.1016/j.apm.2008.01.017

Sharma, B. & Barman, R. N. (2020). Steady laminar flow past a slotted circular cylinder. *Physics of Fluids*, *32* (7), 073605. https://doi.org/10.1063/5.0007958

Shen, P., Lin, L., Wei, Y., Dou, H. & Tu, C. (2019). Vortex shedding characteristics around a circular cylinder with flexible film. *European Journal of Mechanics – B/Fluids*, *77*, 201–210. https://doi.org/10.1016/j.euromechflu.2019.05.008

Shukla, S., Govardhan, R. N. & Arakeri, J. H. (2013). Dynamics of a flexible splitter plate in the wake of a circular cylinder. *Journal of Fluids and Structures*, *41*, 127–134. https://doi.org/10.1016/j.jfluidstructs.2013.03.002

Summary

Simulation of laminar flow passing through a T-splitter plate and bridge pier. The present analysis focuses on the investigation of the two-dimensional flow passing a bridge pier nearby a splitter plate in different regimes of a laminar flow. The splitter plate is T-shaped and two different cases have been studied based on the form of the splitter plate

Qasim, R. M., Jabbar, T. A., Faisal, S. H. (2023). Simulation of laminar flow passing through a T-splitter plate and bridge pier. *Sci. Rev. Eng. Env. Sci*., *32* (2), 135–154. DOI 10.22630/srees.4548

relative to the bridge pier. The analysis is implemented for steady and incompressible water flow in an open channel. The current study deals with velocity vectors, drag coefficients, lift coefficients, and skin friction. The analysis of the velocity vector gave a good indicator about the separation process and dissipation, which occurs at the splitter plate before the occurrence of these processes at the front face of the pier, especially the flow separation process. Moreover, the velocity vector gave a good image about the flow direction at two regions, the first region is located between the rear portion of the splitter plate and the frontal face of the pier, while the second region is the wake region, which is located at the downstream of the pier. Negative drag coefficient, lift coefficient, and skin friction coefficient values are obtained from the analysis. This happens due to the existence of the splitter plate that leads to the reduction of these values.